

## Fabrication of bone phantoms with numerically designed cancellous bone patterns

海綿骨パターンを数値的に生成した骨ファントムの作製

Shohei Nakata<sup>†</sup>, Satoshi Suzuki, Toshihiro Teraoka, Ryouyusuke Fukai, and Masahiro Ohno (Chiba Institute of Technology)

中田晶平, 鈴木悟史, 寺岡俊洋, 深井涼佑, 大野正弘 (千葉工大)

### 1. Introduction

We are attempting to create bone phantoms using 3D printers that can be used as standard samples in bone sonometry experiments<sup>[1,2]</sup>. Our goal is to design and fabricate various bone models the structural parameters of which are controllable. For instance, to simulate the osteoporotic deterioration, it is desirable to prepare such models as the shapes of the cortical part and the trabecular network are unchanged but the BV/TV (bone volume/total volume) values are different. The influence of anisotropy or inhomogeneity of pore structure on ultrasonic propagation can be investigated effectively if such models are produced. Thinkable tactics to design the trabecular structures may include importing and modifying the existing porous materials such as polymer sponges<sup>[1,2]</sup>, and creating the structure by purely numerical calculation as is done for soft tissues<sup>[3]</sup>. In this paper, we report on the latter. In the following, we introduce two designing principles, which we call "continuous field method" and "point-connection method", and the results of 3D printing of designed models.

### 2. Method

#### 2.1. Continuous field method

The data for 3D printing must have the apparent surface of solid. However, in this "continuous field method", we begin with creating a continuous function  $F(x, y, z)$  mimicking the network pattern of the trabecular but having no surfaces. The function  $F(x, y, z)$  is created by superposing Gaussian functions  $f_{(i)}(x, y, z)$ , each of which is centered at  $P_{(i)}(x, y, z) = (s_x^{(i)}, s_y^{(i)}, s_z^{(i)})$ , which corresponds to the position of the pore.

$$F(x, y, z) = \sum_{i=1}^N f_{(i)}(x, y, z)$$

$$= \sum_{i=1}^N \exp \left[ - \left\{ \frac{(x - s_x^{(i)})^2}{r_x^2} + \frac{(y - s_y^{(i)})^2}{r_y^2} + \frac{(z - s_z^{(i)})^2}{r_z^2} \right\} \right]$$

Pore positions  $P_{(i)}(x, y, z)$  are initially set as periodic

lattice points (cubic or hexagonal), and then shifted randomly to some extent. The amount of the random shift, which is represented by the random factor  $RF$  in this article, is determined by computer-generated random numbers. Thresholding or local-minimum detection are performed on  $F(x, y, z)$  to determine the surface position.

Three-dimensional data thus obtained is converted into two-dimensional sliced images (256 or 512 images), which are then processed by the commercial software (*Volume Extractor* (i-plants systems) or *Mimics* (materialise)) to create three-dimensional polygon data.

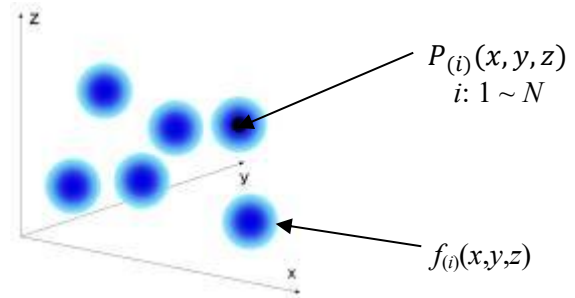


Fig. 1 Continuous field method.

#### 2.2. Point-connection method

Our second approach to design the network structure is rather simple. First we place "node-points" in the  $xyz$  space in the same way we placed  $P_{(i)}(x, y, z)$  in the former section. Then adjacent nodes are connected by straight lines, resulting to give the thinnest trabeculas. Thickening the trabeculas is performed by attaching new solid regions outwards from the solid/liquid interfaces.

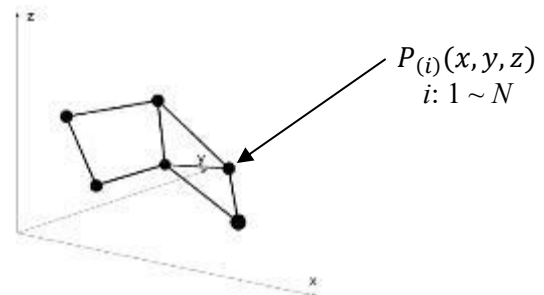


Fig. 2 Point-connection method.

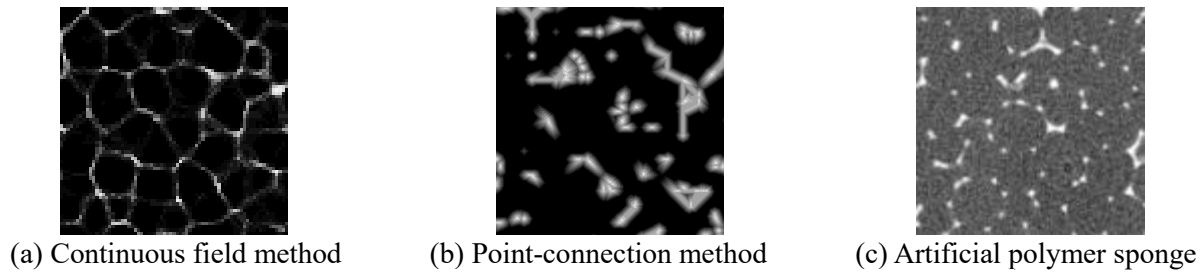


Fig. 3 Two-dimensional images of network structures.

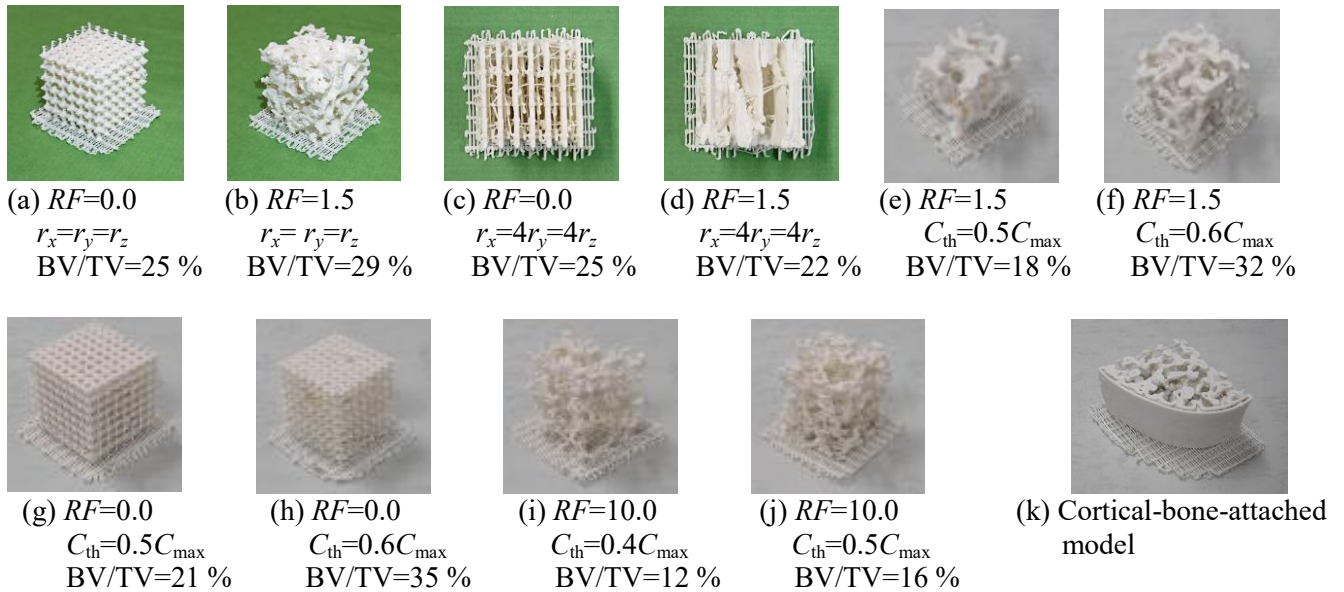


Fig. 4 Bone phantoms fabricated by 3D printers. Models (a)-(f) were designed by continuous field method, whereas (g)-(j) by point-connection method. Model (k) was connected cortical bone and trabecular bone(continuous field method).

### 3. Result

In Fig. 3 we show sliced images of the network structures generated by the continuous field method, the point-connection method, and the artificial sponge. Fig.4 shows the result of 3D printing. The parameter  $C_{\max}$  is the highest value in pre-thresholding gray-scale data, and  $C_{\text{th}}$  is the thresholding value. The BV/TV values were determined by the mass of models and the density of the printing material. Both the continuous field method and the point-connection method could produce network structures. However, the shape of the trabeculas by continuous field method did not become cylindrical but became more wall-like. This was also observed in Fig. 3, in which the structure was depicted as more closed-cell-like in (a), but as open-cell-like in (b) and (c). The point-connection method is free from this “closed-cell” or “wall-like” problems, but on the other hand, it can only produce simple straight-line-connected trabeculas. The BV/TV values of the printed models ranged 15~42% in the continuous field method, and 12~35% in the point-connection method. We need to

extend this value to the lower direction to represent higher osteoporotic states.

### 4. Conclusions

We devised two methods of generating trabecular structures of cancellous bones in a numerical manner in view of making ultrasonometric bone phantoms. Both methods could produce network structures, many problems to be tackled remaining in terms of reproducing the smooth shape of real trabeculas, keeping open-cell structures, and realizing higher osteoporotic states.

### References

1. M. Ohno *et al.*: Proc. Symposium on Ultrasonic Electronics, **36**, Nov 5-7, Tsukuba, Japan, (2015) 1P5-2.
2. S. Nakata *et al.*: Proc. Symposium on Ultrasonic Electronics, **37**, Nov 16-18, Busan, Korea, (2016) 2P5-12.
3. T. Yamaguchi *et al.*: Jpn. J. Appl. Phys. **42** (2003) pp. 3292–3298.